

The Tsunami of 26 December 2004: Numerical Modeling and Energy Considerations

ZYGMUNT KOWALIK, *Institute of Marine Science, University of Alaska*

WILLIAM KNIGHT, *NOAA/NWS/West Coast and Alaska Tsunami Warning Center*

TOM LOGAN, *Arctic Region Supercomputing Center*

PAUL WHITMORE, *NOAA/NWS/West Coast and Alaska Tsunami Warning Center*

Abstract. A numerical model for the global tsunamis computation constructed by Kowalik et al. (2005), is applied to the tsunami of 26 December 2004 in the World Ocean from 80° S to 69° N with spatial resolution of one minute. Because the computational domain includes close to 200 million grid points, a parallel version of the code was developed and run on a Cray X1 supercomputer. An energy flux function is used to investigate energy transfer from the tsunami source to the Atlantic and Pacific Oceans. Although the first energy input into the Pacific Ocean was the primary (direct) wave, reflections from the Sri Lankan and eastern shores of India were a larger source. The tsunami traveled from Indonesia, around New Zealand, and into the Pacific Ocean by various routes. The direct path through the deep ocean to North America carried miniscule energy, while the stronger signal traveled a much longer distance via South Pacific ridges as these bathymetric features amplified the energy flux vectors. Travel times for these amplified energy fluxes are much longer than the arrival of the first wave. These large fluxes are organized in the wave-like form when propagating between Australia and Antarctic. The sources for the larger fluxes are multiple reflections from the Seychelles, Maldives and a slower direct signal from the Bay of Bengal. The energy flux into the Atlantic Ocean shows a different pattern since the energy is pumped into this domain through the directional properties of the source function. The energy flow into the Pacific Ocean is approximately 75% of the total flow to the Atlantic Ocean. In many locations along the Pacific and Atlantic coasts, the first arriving signal, or forerunner, has lower amplitude than the main signal which often is much delayed. Understanding this temporal distribution is important for an application to tsunami warning and prediction.

Key words: Indonesian tsunami, tsunami model, maximum amplitude, energy flux

1. Introduction

To study tsunamis in the World Ocean, we have formulated the vertically integrated equations of motion in spherical polar coordinates (Kowalik et al., 2005). In this numerical approach the higher order of approximation in space for the continuity equation was achieved by expanding the upwind/downwind flux code originally proposed by Mader (2004). For large scale computations an upwind/downwind scheme is essential as it displays strong stability. The integration domain extends from 80° S to 69° N. The boundaries include both wet and dry points. Along the coastal (dry points) the normal velocity is set to zero. At the wet boundary points (along 69° N) the radiation condition, established by Reid and Bodine (1968) is used. The entire globe is cut along 20° E longitude, requiring a cyclic boundary condition for sea level and the E-W velocity on this meridian. It appears at first glance that the above boundary conditions are sufficient to derive a solution. Early numerical experiments however, show that even with the relatively large space step of $1'$, new dry and wet points may be generated due to runup or run-down. A numerical scheme for wetting and drying needs to be introduced. The total water depth is the parameter usually tested to detect the presence of wet or dry points (Flather and Heaps, 1975; Imamura, 1996; and Kowalik and Murty, 1993b). Wet and dry points are identified by

setting the average (undisturbed) ocean depth as positive (wet points) and elevations (dry points) as negative values. The total water depth in the dry grid points is taken as zero.

The spatial grid step of numerical computation is 1' (1minute equals to 1.852km at the equator), and its length changes along the circle of latitude. The total number of the grid points is close to 2×10^8 , therefore the simple time stepping solution, even on a supercomputer, takes several weeks. The entire domain was split along meridians into 60 subdomains to apply 60 processors. With this parallelization, 50hrs of tsunami propagation was reproduced in 9hrs of a CRAY X1.

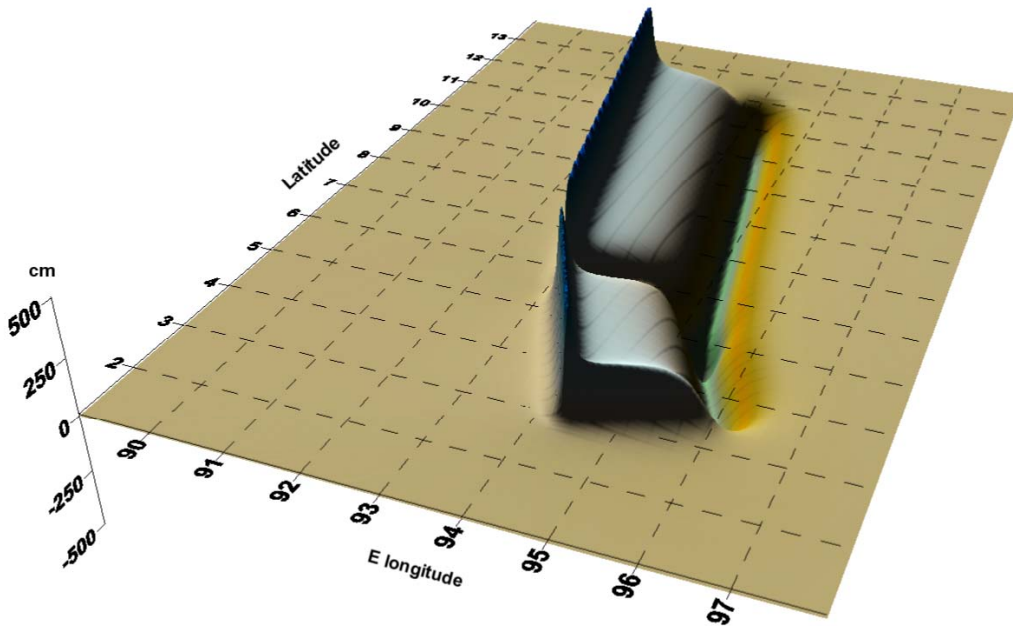


Figure 1. The source function for the tsunami of 26 Dec.2004.

A small spatial step is important as short-period waves can be obliterated during large propagation distances when large spatial steps are used. Taking the average depth of the World Ocean as 4000 m, a wave with 10 minute period has a wavelength close to 120km. This wave length is discretized by a 1' grid into about 64 mesh lengths. The amplitude of a sinusoidal wave propagating over 10000km will diminish only about 2%, and some shorter dispersive waves will be generated as well (Kowalik, 2003).

The details of the source function construction and geographical distribution is given in Kowalik et al., (2005). Permanent, vertical sea floor displacement is computed using the static dislocation formulae from Okada (1985). The generation mechanism for the Indian Ocean tsunami is mainly the static sea floor uplift caused by abrupt slip at the India/Burma plate interface. To accommodate trench curvature, the fault plane is broken into two segments. Maximum uplift is 507cm and maximum subsidence approximately 474cm. The 3-D rendering of the source function is shown in Figure 1.

The major conclusion in Kowalik et al., (2005) was that in the Pacific Ocean, those stations located in the Northern Pacific show the largest differences between calculated and observed travel time. This is caused either by a small tsunami signal to noise ratio or by multiple paths from the source to gauge locations. In the latter case, especially important is an interaction of the higher energy tsunami signals which travel slowly over the oceanic ridges and the lower energy signals which travel faster over the deep oceanic regions. In the present paper we follow the changes in tsunami signal as it traveled from Indonesia to the Pacific Ocean. The tsunami energy

flux is the investigative tool used for this purpose.

2. Global distribution of maximum amplitude

Model computations using the above source were made for 50 hrs of propagation, allowing the tsunami signal to travel over the entire World Ocean. During this computation the maximum tsunami amplitude in every grid point was recorded. The plot of maximum amplitude in the proximity of the generation domain is shown in Figure 2 and the corresponding plot for the World Ocean is shown in Figure 3.

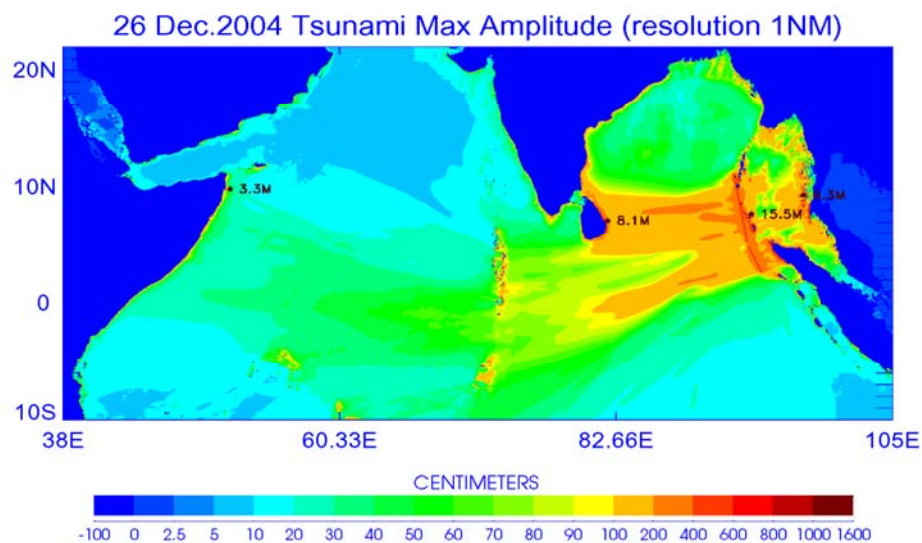


Figure 2. Maximum modeled tsunami amplitude in the Indian Ocean.

The strongly directional signal generated by the elongated source dominates the Indian Ocean domain. The main energy lobe is directed towards Sri Lanka and the secondary lobe points towards South Africa, sending a strong signal into the Atlantic Ocean.

The global maximum amplitude distribution (Figure 3) shows that the Indonesian tsunami traveled all over the World Ocean. Although the source directivity pushed most of the wave energy towards southern Africa, a strong signal is nonetheless directed towards Antarctica. It is easy to see by checking the bathymetry that the tsunami tended to propagate towards Antarctica along the oceanic ridges and subsequently continued to transfer higher energy along the South Pacific ridge towards South and Central America. This mode of propagation brings the modeled tsunami amplitude up to 65cm along the Pacific coast of South America. A similar mode of energy transfer is observed in the Atlantic, where the Mid-Atlantic Ridge channels the tsunami to produce 30cm amplitude as far north as Nova Scotia. This figure also depicts the amplitude enhancement in shallow water and especially in proximity to peninsulas and islands due to energy concentration through refraction.

An especially large energy flux is ducted from the South Atlantic Ridge towards Brazil and Argentina. The filaments of energy trapped along the South Pacific Ridges are most spectacular as they duct tsunami energy for many thousands of kilometers. A simple explanation of the

energy trapping using the continuity equation leads us to conclude that amplitude should increase over the ridges due to shallower depth. At the same time, the role of bottom friction over the 3km

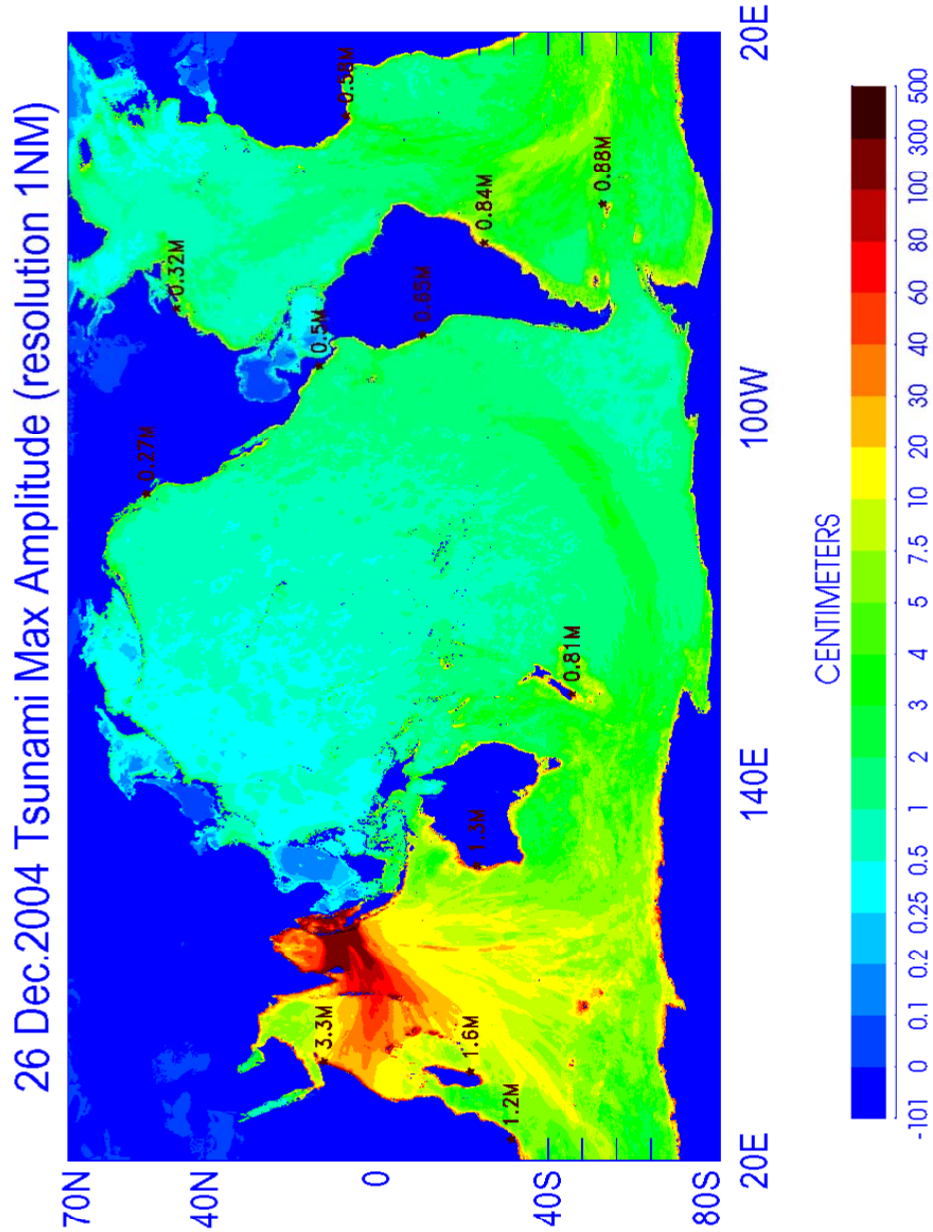


Figure 3. Maximum modeled tsunami amplitude in the World Ocean

deep ridge is negligible and therefore the tsunami can travel long distance without energy losses. To demonstrate the pattern of the energy trapped over the various bathymetric features we introduce the energy flux. In the rectangular system of coordinates, with the x coordinate along E-W direction and y along N-S direction, the u component of velocity along x direction can be combined with the sea level (ζ) to define E-W component of the energy flux vector (Kowalik and Murty, 1993a):

$$E_x = \rho g H u \zeta \quad (1)$$

Similarly, the N-S component of the energy flux vector is defined (with v , the velocity

component along the y direction):

$$E_y = \rho g H v \zeta \quad (2)$$

In the above: ρ is the sea water density, $g = 9.81 \text{ m s}^{-2}$ is the Earth's gravity acceleration and H is the ocean depth. The energy flux vector for the progressive wave is always propagating into the same direction as the sea level and velocity and its direction is perpendicular to the wave front. To preserve direction of the energy flux in the progressive wave the velocity and sea level elevation remain in phase (Henry and Foreman, 2001). Energy flux units are expressed as Joule/(s cm) so this is an energy flux per unit width and per unit time. To derive the total energy flux the above expressions should be multiplied by the length of a crosssection and integrated over the time period.

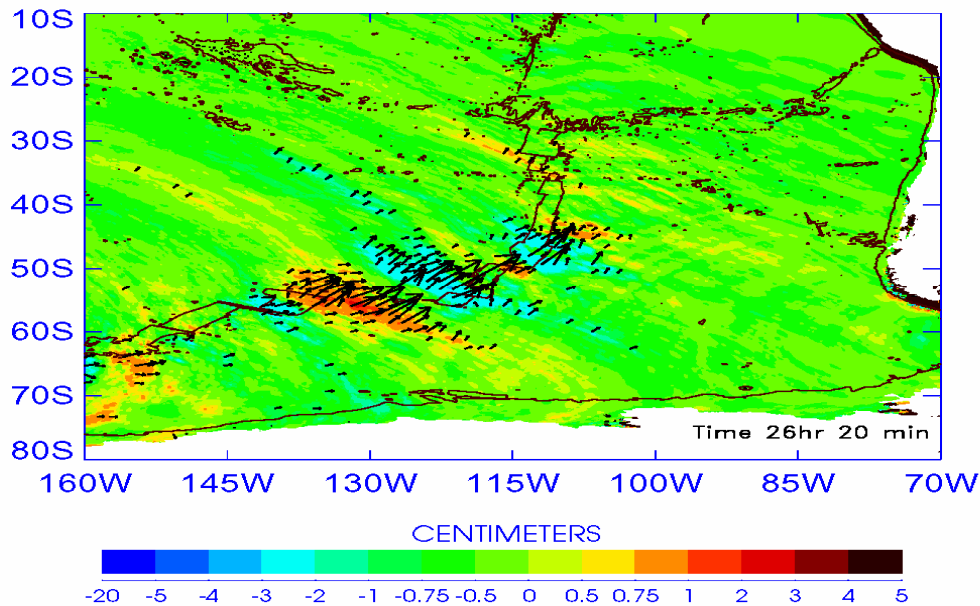


Figure 4. Energy flux vectors over the South Pacific Ridge at time 26 hr 20 min. The colors denote the sea level. The dark-brown lines denotes the ridge depth - 3000m depth contour.

In Figure 4 the energy flux vectors are shown in the south-western part of the Pacific Ocean. The larger tsunami amplitudes are located above the oceanic ridge and the energy flux is directed along the ridge. This small group of higher amplitude waves does not belong to the first tsunami signal to arrive in this region. Its average wavelength is about 1350km, as the depth of the ridge is close to 3km the wave period is about 2 hrs. This is a somewhat long period for a tsunami. The wave pattern also shows that the waves over ridges are slower than the off-ridge waves, suggesting trapping due to refraction and focusing of off-ridge energy towards the ridge. Nonetheless we cannot exclude the possibility of a resonance interaction of the tsunami wave and ridge bathymetry since Snodgrass et al., (1962) demonstrated the presence of discrete spectra in waves trapped over depth discontinuities. Mei (1989) showed that over a stepped bottom ridge the discrete spectra exist as well. If an incident wave can excite these trapped modes, an amplification of the tsunami signal due to resonance will follow.

3. Time dependent propagation

Although the maximum amplitude defines tsunami distribution in the World Ocean, it does not

reveal the temporal development of tsunamis. To improve understanding of the large scale temporal processes we use the temporal change of the tsunami energy fluxes passing through various crosssections. The first crosssection is considered in the Indian Ocean, from 80° E to 105° E along 10° S (see Figure 2). The southward directed energy flux shown in Figure 5 is responsible for the tsunami

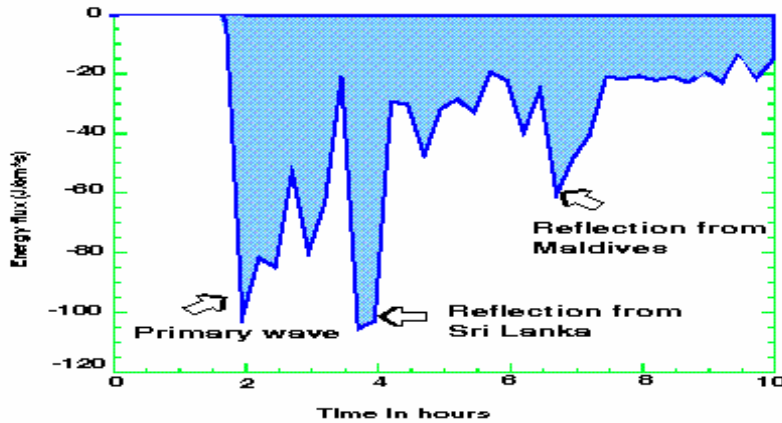


Figure 5. Southward directed energy flux through the E-W crosssection located in the Indian Ocean along 10° S from 80° E to 105° E.

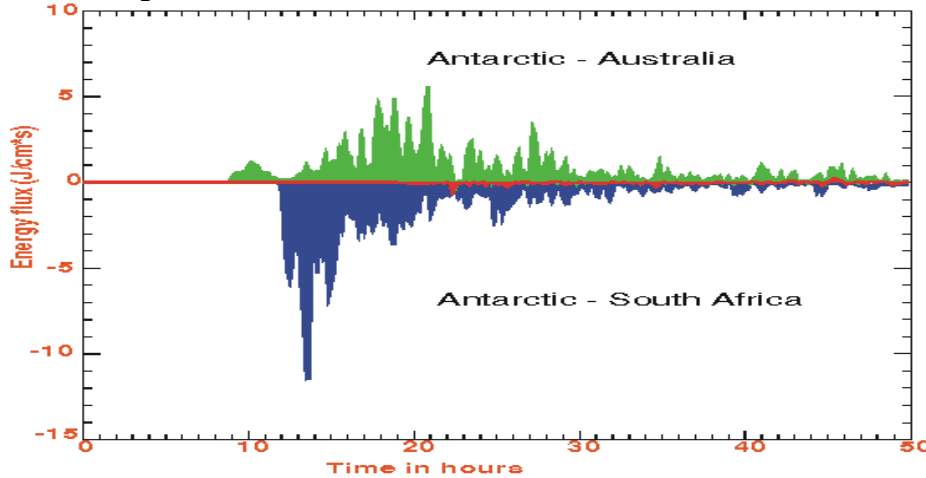


Figure 6. Energy flux through the crosssections located between Antarctic and major continents. Along 20° E from Antarctica to South Africa, blue color; along 140° E, from Antarctic to Australia, green color, along 70° W from South America and Antarctic, red color.

signal propagating into the Pacific. The first maximum in this figure has been associated with the direct wave passing through the latitude 10° S at 2hrs after the initial source motion. The next, even bigger energy influx arrives 2 hrs later, and is caused by the reflection from Sri Lanka and the east coast of India. The reflection from the Maldives Islands generates a signal which passes the crosssection at about 6.5 hrs from the initial disturbance. This crosssection is located quite close to the Bay of Bengal and therefore a large portion of the Maldives-reflected signal omits this route. Since the Bay of Bengal acts as a parabolic mirror, it sends many reflected signals of smaller amplitude southward. The conclusion from the above experiment is that the reflected signal may send more energy south than the direct signal.

With the major maxima in the southward directed signal identified, the task to associate them with the signal propagating into the Pacific Ocean remains. For this purpose an energy flux is considered through the three crosssections located between Antarctica and the major continents. The crosssection (blue color in Figure 6) along the longitude 20E from Antarctica to South Africa (AS) shows the time variation of the energy flux between Indian and Atlantic Oceans. This flux remains negative for the entire period of 50 hrs, thus confirming that the inflow is directed into the Atlantic Ocean. On the other hand the energy flow through a crosssection along 140E (green color in Figure 6) from Antarctic to Australia (AA) is at all times positive (from the Indian to Pacific Oceans). The flux through the crosssection located between South America and Antarctica at 70W (red color in Figure 6), reveals a small in-flow from the Atlantic into the Pacific. Figure 6 clearly demonstrates that the magnitude and the time variability of energy fluxes through crosssections AA and AS are quite different in character. The flux passing AS has a large value and the maximum energy inflow to the Atlantic is located close to the initial wave front, even though the first arriving signal is not related to the maximum energy. The energy flow into the Atlantic is a result of the source orientation as shown in Figure 2. The main energy maximum is slower to arrive than the initial signal because, as Figure 3 suggests, the maximum energy directed towards SA crosssection is located along the oceanic ridge. Due to smaller depth over this ridge the more energetic signal propagates slower. The energy flow through AA demonstrates that tsunami arrives about 10 hrs from the onset of the earthquake; it initially has a small amplitude which slowly increases in time to achieve a few maxima from 18 to 21 hrs. To understand the origin of this complicated temporal pattern of energy flux through AA we turn to Figure 5 and analyze the southward energy flux from the source area. The first signal arriving at the southern boundary in Figure 5 also crosses AA as the initial signal, since the travel time for this signal is close to 10hrs. The second signal arriving two hours later is caused by the reflection from the Sri Lanka and Indian coasts. The maxima in Figure 6 occurring from 18 to 21hrs are related to the energy flux arriving by the various routes from the Indian Ocean. The arrival time of these signals depends on the depth and on the traveled distance. Therefore, it is useful to notice that the route from the generation domain to South America via passages between Australia and Antarctic is the great circle of a sphere. Signals which travel from the generation area to the section AA through the deep ocean travel faster, in about 10hrs, but they transfers less energy. The slower signal travels along oceanic ridges and transfers more energy as confirmed in Figure 4 by the energy flux vectors. This appears to be only a part of the story. Tracking (through animations) the signal shown in Figure 4 backwards, the tsunami passes between Australia and Antarctica, as depicted in crosssection AA (Figure 5) and then loses its identity going back into southern Indian Ocean. The large inflow of energy shown in Figure 4, is related to the reflected signals off the Seychelles, Maldives and Africa and to a slowly traveling tsunami which originated in the Bay of Bengal. The passage between Antarctica and Australia/New Zealand plays a large role in signal amplification. As the passage is wide on the Indian Ocean side and constrained on the Pacific side, the eastward moving signal is amplified and is also reorganized into periodic wave-like structures. A similar reorganization of a quasi-turbulent signal into oscillatory wave pattern can be observed in the passage between South America and Africa for the tsunami propagating from the Southern into the Northern Atlantic.

To compare the total energy flux entering Pacific and Atlantic Oceans over the 50hrs of process, the energy fluxes given in Figure 6 have been integrated in time. The total energy flowing into the Pacific Ocean is approximately 75% of the total flow to the Atlantic Ocean.

4. Observations versus computations

Although the 1' computational mesh resolves many coastal and bathymetric features, nonetheless

it is too large to resolve the local dynamics such as runup. In Figure 7, four stations have been chosen from the Indian Ocean area and are compared with observations described by Merrifield et al., (2005).

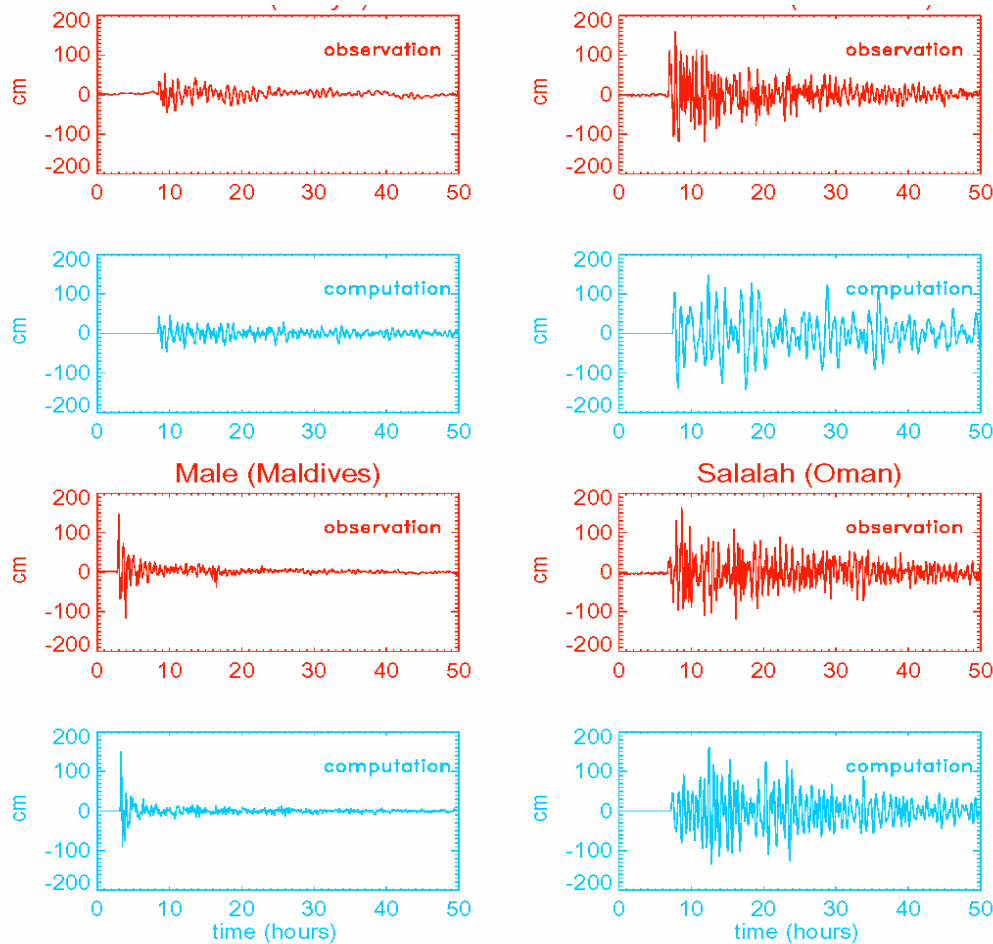


Figure 7. Observations and computations from the four stations in the Indian Ocean.

The stations are located on Maldives Island (Male), on the Seychelles Islands (Pt LaRue), on the African coast of Kenya (Lamu) and on the Arabian Peninsula coast of Oman (Salalah). The model reproduces quite well the maximum amplitude and the temporal behavior of the tsunami, indicating that with higher resolution bathymetry an even better comparison can be achieved. As luck would have it, Jason-I altimetry satellite traversed the Indian Ocean about 2 hours after the event origin time. It crossed the equator on a NNE path at 02:55 UTC on 12-26-2004 (Figure 8). The non-validated altimetry data was downloaded from the JPL Physical Oceanography website at ftp://podaac.jpl.nasa.gov/pub/sea_surface_height/jason/j1nrtssh/data/. Altitude is sampled approximately once per second and is corrected for tides. In order to remove any background, the raw data from the “tsunami pass” was corrected by subtracting out an average of 4 “non-tsunami” passes. Jason-I repeats its track about once every ten days, so four repeat paths were averaged to generate the background. The corrected signal, was then smoothed by removing fluctuations with wavelengths shorter than 20km. The smoothed signal with background removed was compared against the model data. Note that Jason-I was above the tsunami for about ten minutes. During this time the tsunami was in motion, so the comparison is made to dynamic model predictions and not against a static snapshot.

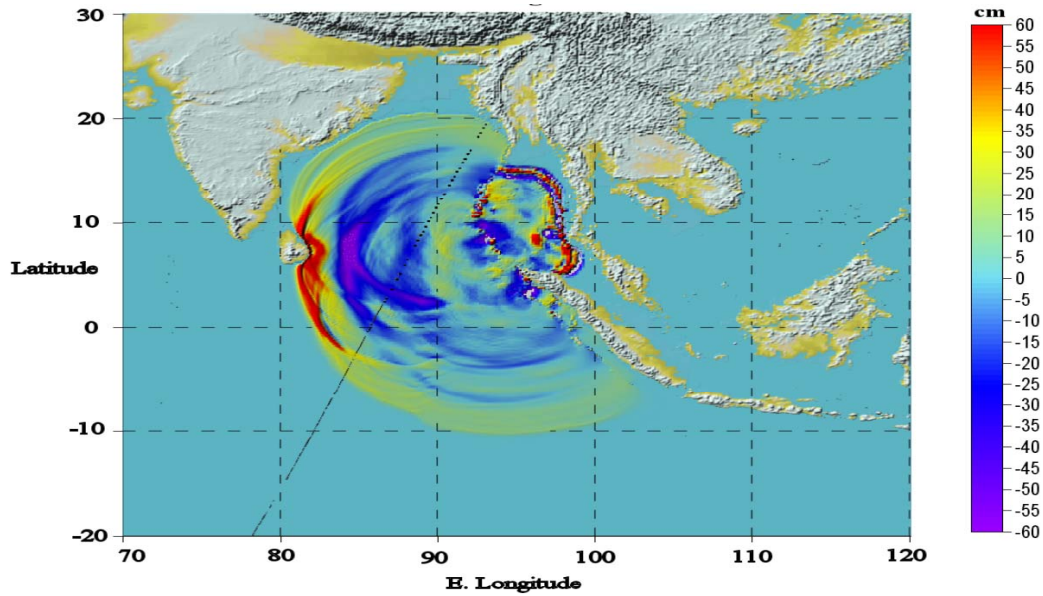


Figure 8. Ground track of Jason-I and computed tsunami amplitude at 2:55 UT on Dec. 26, 2004 in the Indian Ocean.

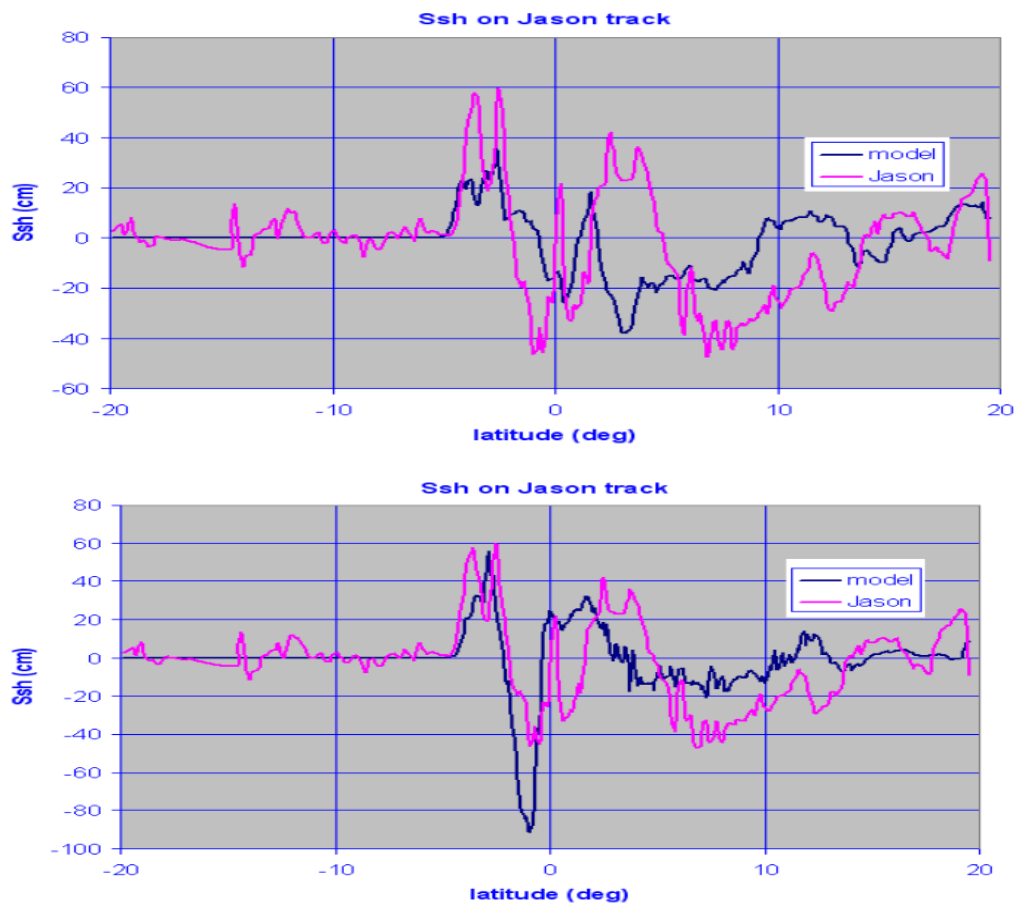


Figure 9. Computed and observed tsunami amplitude along the Jason-I track. Upper panel: source function given in Figure 1. Lower panel: source function orientation and width adjusted.

The model wave heights at the moment of equatorial crossing are shown in Figure 8. Jason-I crosses the leading edge wave at a point on the wave front where the amplitude is rapidly increasing towards the NW. The comparison between data and model is therefore sensitive to small variations in source details. The final comparison is shown in figure 9 (upper panel). The leading edge wave location is predicted accurately by the model, even if the amplitude is not. The modeled leading wave with the amplitude similar to the recorded by satellite was in the satellite footprint 15 min earlier (see, Figure 8). A closer amplitude/period match was obtained by rotating the source strike counterclockwise slightly, and by reducing the fault width from 200km to 125km. The comparison, given in Figure 9 (lower panel) shows that the model as driven by the adjusted source function reproduces more accurately the leading wave recorded by Jason-I.

5. Discussions and conclusions

The main purpose of the present paper was to derive a global picture of the Indonesian tsunami based on a computer model. By comparison to the global observation we hope to identify major patterns of tsunami propagation. Computed distributions of the maximum amplitude compare well with observations analyzed by Merrifield et al., (2005) and by Rabinovich (2005). The observed and computed temporal variation of the tsunami at gauge stations in the Indian Ocean display quite similar amplitude and variability, although the model resolution of about 2km still needs to be improved for proper runup calculations. The comparison against satellite data shows that improvements in the source function are needed. The source location was constrained by tsunami travel times to tide gauge locations and by earthquake parameters computed from seismic data inversions (see, Kowalik, et al., 2005). Further investigation through comparison to the magnitude and location of the satellite signal should also improve the source parameters.

The model computations reveal peculiarities of tsunami signal when it travels from the source over entire World Ocean. The most interesting is ducting the tsunami energy along oceanic ridges which is so clearly shown in Figures 2 and 3. To demonstrate the pattern of energy trapping over the ridges, the energy flux function is used. The energy flux vectors show magnification over the South Pacific Ridge and their distribution suggest trapping due to refraction and focusing the off-ridge energy towards the ridge.

Further investigations of energy fluxes show more complicated temporal and spatial patterns in tsunami propagation. The primary signal traveling towards the Pacific Ocean depicted the low energy level, therefore it was not well observed at the sea level gauges. The more energetic signal arrived with some delay. The investigation of the energy flux along the South Pacific Ridge reveals tsunami of approximately 2 hrs period. Tracking (through animations) tsunamis passing between Australia and Antarctica we have found that the signal moving from west to east is amplified and is also reorganized into periodic wave-like structures. Similar reorganization of the tsunami occurs between South America and Africa for the tsunami propagating from the Southern into the Northern Atlantic.

References

Flather, R.A. and Heaps, N.S.: 1975, Tidal computations for Morecambe Bay. *Geophys. J. Royal*

Astr. Soc., **42**, 489-517.

Gover, J.: 2005, Jason 1 detects the 26 December 2004 tsunami, *EOS, Trans. AGU*, **86**, 37-38.

Henry, R.F. and Foreman M.G.G.: 2001, A representation of tidal currents based on energy flux, *Marine Geodesy*, **24**(3), 139-152.

Imamura, F.: 1996, Review of tsunami simulation with a finite difference method. In *Long-Wave Runup Models*, H. Yeah, P. Liu and C. Synolakis, Eds, World Scientific, 25-42.

Kowalik, Z.: 2003, Basic Relations Between Tsunami Calculation and Their Physics - II, *Science of Tsunami Hazards*, **21**(3), 154-173

Kowalik, Z. and Murty, T.S.: 1993a, *Numerical Modeling of Ocean Dynamics*, World Scientific, 481 pp.

Kowalik, Z. and Murty, T.S.: 1993b, Numerical simulation of two-dimensional tsunami runup. *Marine Geodesy*, **16**, 87-100.

Kowalik, Z., Knight, W., Logan, T., and Whitmore, P.: 2005, NUMERICAL MODELING OF THE GLOBAL TSUNAMI: Indonesian Tsunami of 26 December 2004. *Science of Tsunami Hazards*, **23** (1), 40-56

Mader, C. L.: 2004, *Numerical Modeling of Water Waves*, CRC Press, 274 pp.

Mei, C. C.: 1989, *The Applied Dynamics of Ocean Surface Waves*, World Scientific, 740 pp.

Merrifield, M.A., Y.L. Firing, T. Aarup, W. Agricole, G. Brundrit, D. Chang-Seng, R. Farre, B. Kilonsky, W. Knight, L. Kong, C. Magori, P. Manurung, C. McCreery, W. Mitchell, S. Pillay, F. Schindele, F. Shillington, L. Testut, E.M.S. Wijeratne, P. Caldwell, J. Jardin, S. Nakahara, F.-Y. Porter, and Turetsky, N.: 2005, Tide Gauge Observations of the Indian Ocean Tsunami, December 26, 2004, in press, *Geophysical Research Letters*, **32**.

Okada, Y.: 1985, Surface deformation due to shear and tensile faults in a half-space, *Bulletin of the Seismological Society of America*, **75**, 1135-1154.

Rabinovich, A.B. 2005. Web compilation of tsunami amplitudes and arrival times. http://www-sci.pac.dfo-mpo.gc.ca/osap/projects/tsunami/tsunamiasia_e.htm.

Reid, R.O. and Bodine, R.O.: 1968, Numerical model for storm surges in Galveston Bay. *J. Waterway Harbor Div.*, **94**(WWI), 33-57.

Snodgrass, F.E., Munk, W.H. and Miller, G. R.: 1962, California's continental borderland. Part I. Background spectra. *J. Mar. Research*, **20**, 3-30.